Journal of Fluorescence, Vol. 3, No. 1, 1993

Distance Distributions and Dynamics of a Zinc Finger Peptide from Fluorescence Resonance Energy Transfer Measurements[1]

Peggy S. Eis,[1,2] Józef Kuśba,[2,3] Michael L. Johnson,[4] and Joseph R. Lakowicz[2,5]

Received July 24, 1992; revised June 16, 1993; accepted June 24, 1993

Time-resolved fluorescence resonance energy transfer (FRET) measurements were used to measure distance distributions and intramolecular dynamics (site-to-site diffusion) of a 28-residue single-domain zinc finger peptide in the absence and presence of zinc ion. Energy transfer was measured between TRP_{14} and a N-terminal DNS group. As expected, the TRP-to-DNS distance distribution for zinc-bound peptide is shorter and narrower (R_{av} = 11.2 Å, hw = 2.8 Å) than the metal-free peptide (R_{av} = 20.1 Å, hw = 14.5 Å). The degree of mutual donor-to-acceptor diffusion (D) was also determined for these distributions. For zinc-bound peptide there is no detectible diffusion ($D \leq 0.2$ Å^2/ns), whereas for metal-free peptide a considerable amount of motion is occurring between the donor and the acceptor (D = 12 Å^2/ns). These results indicate that the zinc-bound peptide folds into a unique, well-defined conformation, whereas the metal-free conformation is flexible and rapidly changing. The absence of detectible mutual site-to-site diffusion between the donor and the acceptor in the metal-bound zinc finger peptide indicates that intramolecular motion is essentially frozen out, on the FRET time scale, as a consequence of zinc coordination.

KEY WORDS: Zinc finger peptide; distance distributions; dynamics; frequency-domain fluorometry.

INTRODUCTION

Zinc finger proteins are a class of proteins which tetrahedrally coordinate zinc ion via cysteine (C)[6] and histidine (H) residues [1–3]. Eukaryotic transcription factors, a subclass of zinc finger proteins, are DNA-binding proteins containing multiple CCHH zinc-binding domains [4]. Single-domain zinc finger peptides have been synthesized to characterize the properties of this metal binding structure. These peptides fold into a unique structure in the presence of metal ion [3, 5–17]. A three-dimensional structure was predicted by Berg [18] and recent NMR-determined structures [6, 8, 10, 13, 14], as well as a crystallographic structure [19], have been found to be very similar to this predicted structure.

Since NMR and crystallographic methods are lim-

[1] Dedicated to the memory of Barbara D. Wells.

[2] Center for Fluorescence Spectroscopy, Department of Biological Chemistry, University of Maryland, School of Medicine, 108 North Greene Street, Baltimore, Maryland 21201.

[3] Permanent address: Technical University of Gdańsk, Department of Technical Physics and Applied Mathematics, 80-952 Gdańsk, Poland.

[4] Department of Pharmacology, University of Virginia, Charlottesville, Virginia 22908.

[5] To whom correspondence should be addressed.

[6] Abbreviations used: C, cysteine; H, histidine; NMR, nuclear magnetic resonance; D, donor; A, acceptor; Fmoc, *N*-fluorenylmethoxycarbonyl; FRET, fluorescence resonance energy transfer; DNS, 5-dimethylamino-1-naphthalene sulfonyl; DTT, dithiothreitol; TRP, tryptophan or tryptophan residue; hw, full width at half-maximum probability of the distance distribution; R_{av}, maximum probability distance of the distribution; ZF_{28}, zinc finger peptide with 28 amino acids and a consensus sequence; TFA, trifluoroacetic acid.

1053-0509/93/0300-0023$07.00/0

ited in their ability to look at unstable protein structures or detect large structural changes, we decided to examine the metal-free and metal-bound states of a single-domain zinc finger peptide with time-resolved fluorescence resonance energy transfer (FRET) methods. Our measurements enable us to calculate the distribution of distances between two sites (donor-to-acceptor) within the molecule [20–28]. These distributions reveal both the average donor–acceptor distance and the range of conformations that exist in solution, as observed from the width of the donor-to-acceptor distance distribution. Additionally, we are able to recover the apparent site-to-site diffusion coefficient [21, 22, 29–33], which enables us to determine the flexing motion that occurs between two sites in the zinc finger peptide.

We synthesized a consensus single-domain zinc finger peptide for our measurements. The consensus peptide's sequence was devised based on the work of Berg and co-workers [17]. Their peptide, which consists of the most frequently occurring residue at each position in the sequence based on the catalogued sequences of other known CCHH zinc fingers, was shown to bind metal ion in a manner similar to native sequence single-domain zinc fingers. We measured the donor-to-acceptor distance distributions of this peptide with and without zinc ion and also determined the distributions with the inclusion of a diffusion parameter, which accounts for intramolecular diffusion between the donor and the acceptor.

THEORY

Energy transfer distance distributions can be determined by measuring the decay emission of the donor in the absence [I_D (t)] and presence [I_{DA} (t)] of acceptor. In our system the emission of both the donor-alone and the donor–acceptor (D-A) pair molecules exhibit complex intensity decays. The lifetimes of the donor-alone are recovered using a multiexponential description of the decay as follows:

$$I_D(t) = I_{D0} \sum_i \alpha_{Di} \exp(-t/\tau_{Di}) \qquad (1)$$

where I_{D0} is the initial ($t = 0$) intensity, α_{Di} are the initial relative fractional intensities of the decay, $\Sigma\alpha_{Di} = 1.0$, and τ_{Di} are the decay times. The lifetimes of the donor–acceptor pair can also be analyzed by the multiexponential model,

$$I_{DA}(t) = I_{DA} \sum_i \alpha_{DAi} \exp(-t/\tau_{DAi}) \qquad (2)$$

where I_{DA} is the initial intensity ($t = 0$), α_{DAi} are the preexponential factors, $\Sigma\alpha_{DAi} = 1.0$, and τ_{DAi} are the apparent decay times. Such an analysis of the intensity decay of the donor–acceptor pair is informative regarding the shape of the donor decay. However, such an analysis does not directly reveal the shape of the distance distribution.

In our analysis of the donor intensity decays, we consider how the presence of the acceptor alters the decay of the donor. We assume that the only mechanism of quenching is by energy transfer from donor to acceptor. Because the decay of the donor is multiexponential even in the absence of acceptor, it is necessary to consider how energy transfer affects each component in the decay. We assume that the components behave as if they each had the same Förster distance (R_0) for transfer. Thus, for the ith component of molecules containing a donor and an acceptor separated by a distance r, the transfer rate is described by

$$k_{Ti} = \frac{1}{\tau_{Di}} \left(\frac{R_0}{r}\right)^6 \qquad (3)$$

where the subscript i represents each individual component. The Förster distance (R_0) is the critical distance at which the rate of energy transfer is equal to the inverse of the respective decay time and is determined from the spectral properties of the chromophores [34].

The observed donor decay from the D-A pairs contains contributions from all components with all allowable distances and will be multiexponential since particular molecular configurations cannot be uniquely examined in solution. Thus, the multiexponential donor decay is given by the average of the individual decays, $\bar{N}_i^*(r, t)$, which are weighted by their fractional intensity (α_{Di}) and by the distance probability distribution, $P(r)$, of the D-A pairs,

$$I_{DA}(t) = I_{DA0} \sum_i \alpha_{Di} \int_{r_{min}}^{r_{max}} P(r)\bar{N}_i^*(r,t)\, dr \qquad (4)$$

We note that, in the absence of donor quenching by factors other than FRET, $I_{DA0} = I_{D0}$. The individual decay of the ith component, $\bar{N}_i^*(r, t)$, is defined as follows:

$$\bar{N}_i^*(r,t) = N_i^*(r,t)/N_{i0}^*(r) \qquad (5)$$

where $N_i^*(r, t)$ is the actual distribution of excited molecules over distance r and $N_{i0}^*(r)$ is the initial distribution of excited moleules. We assume that the shape of the initial distribution [$N_{i0}^*(r)$] is the same for all donor fractions, i.e., $N_{i0}^*(r) = N_{i0}^* P(r)$, where N_{i0}^* is the total initial number of molecules of the ith compo-

nent and $P(r)$ is the probability density function describing the distribution of D-A distances. We assume that $P(r)$ is a bounded Gaussian, and it is given by

$$P(r) = \begin{cases} \frac{1}{Z}\exp\left(-\frac{(r-R_{av})^2}{2\sigma^2}\right) & \text{for } r_{min} \le r \le r_{max} \\ 0 \quad \text{elsewhere} \end{cases} \quad (6)$$

where Z is the normalization factor,

$$Z = \int_{r_{min}}^{r_{max}} \exp\left(-\frac{(r-R_{av})^2}{2\sigma^2}\right) \quad (7)$$

The average distance and standard deviation of the bounded Gaussian function are R_{av} and σ, respectively. The width of the distribution, which represents the degree of conformational flexibility between the donor and the acceptor, is reported as the half-width (*hw*; full width at half-maximum probability). For a Gaussian model $hw = 2.355\sigma$.

In the case where there is no site-to-site diffusion between the donor and the acceptor, the decay $\overline{N}_i^*(r, t)$ is given by

$$\overline{N}_i^*(r,t) = \exp\left[-\frac{t}{\tau_{Di}} - \frac{t}{\tau_{Di}}\left(\frac{R_0}{r}\right)^6\right] \quad (8)$$

It has been shown by Haas and co-workers [21, 27] that in the presence of energy transfer and site-to-site diffusion (D), the function $\overline{N}_i^*(r, t)$ satisfies the diffusion equation with an additional sink term, which takes into account the processes of donor decay and energy transfer,

$$\frac{\partial \overline{N}_i^*(r,t)}{\partial t} = -\left[\frac{1}{\tau_{Di}} + \frac{1}{\tau_{Di}}\left(\frac{R_0}{r}\right)^6\right]\overline{N}_i^*(r,t) + \frac{1}{N_{i0}^*(r)}\frac{\partial}{\partial r}\left[N_{i0}^*(r)D\frac{\partial \overline{N}_i^*(r,t)}{\partial r}\right] \quad (9)$$

For a more thorough description, see Refs. 30–33. A detailed description of the numerical methods used to solve this equation is now available [35].

The frequency-domain data were analyzed by the method of nonlinear least squares [36, 37], as applied to the frequency-domain data [38-39]. This is accomplished by comparison of the values of the observed phase (φ_ω) and modulation (m_ω), at various light modulation frequencies (ω), with those values calculated (c) for various assumed models and parameters ($\varphi_{\omega c}$ and $m_{\omega c}$). These values are obtained by

$$N_\omega = \frac{1}{J}\int_0^\infty I(t)\sin \omega t\, dt \quad (10)$$

$$D_\omega = \frac{1}{J}\int_0^\infty I(t)\cos \omega t\, dt \quad (11)$$

using $J = \int_0^\infty I(t)dt$,

$$\varphi_\omega = N_\omega/D_\omega \quad (12)$$

$$m_{\omega c} = (N_\omega^2 + D_\omega^2)^{1/2} \quad (13)$$

The parameter values determine the precise form of $I(t)$ and are determined by minimization of the goodness-of-fit parameter,

$$\chi_R^2 = \frac{1}{\nu}\sum_\omega\left(\frac{\varphi_\omega - \varphi_{\omega c}}{\delta\omega}\right)^2 + \frac{1}{\nu}\sum_\omega\left(\frac{m_\omega - m_{\omega c}}{\delta m}\right)^2 \quad (14)$$

where $\delta\phi$ and δm are the experimental uncertainties in the phase and modulation, respectively. The number of degrees of freedom (ν) is given by $\nu = 2N - n - 1$, where N is the number of frequencies (ω), and n is the number of free parameters in the fit.

EXPERIMENTAL PROCEDURE

The 28-residue CCHH consensus zinc finger peptice (ZF_{28}) was synthesized on a Milligen 9050 Pepsynthesizer using *N*-fluorenylmethoxycarbonyl (Fmoc) chemistry (see Scheme I for the sequence). Peptides were purified, before and after labeling with 5-dimethylamino-1-naphthalene sulfonyl chloride (DNS-Cl), by HPLC on a Vydac C_4 column with 0.1% TFA in water and 0.1% TFA in acetonitrile. Details of the peptide cleavage and dansylation reactions were described previously [40].

Amino acid analysis and mass spectrometry were

A D

DNS—P Y E C P E C G R S F S Q W S D L T R H Q R T H T G E K

↑ ↑ ↑ ↑

Scheme I. ZF_{28} sequence showing tryptophan donor (W) and dansyl acceptor (DNS).

performed to confirm the unlabeled peptide's sequence. Mass spectrometry was also used to confirm that ZF_{28} was singly labeled with DNS acceptor. Absorption spectra of cobalt-bound ZF_{28} (data not shown) were performed to ensure that it tetrahedrally coordinated metal ion [3].

Fluorescence measurements were performed at 20°C on samples dissolved in 50 m*M* 4-(2-hydroxyethyl)-1-piperazineethane sulfonic acid (HEPES), 50 m*M* NaCl, 10 m*M* dithiothreitol (DTT), pH 7 buffer. Steady-state emission spectra were measured on a SLM 8000 fluorometer and are uncorrected since the instrument response function was relatively unchanged in the tryptophan emission region. The excitation bandwidth was 4 nm, the emission bandwith was 8 nm, and the spectra were collected under magic-angle (54.7°) polarization conditions. The quantum yield of the donor was measured relative to the value of tryptophan in water (0.13) [41]. A κ^2 value of 2/3 was used to calculate the R_0 value. Time-resolved frequency-domain measurements were performed on the instrument described previously [42]. Magic-angle conditions were used for the intensity decay measurements. The excitation source was a rhodamine 6G dye laser frequency-doubled to 295 nm. Tryptophan emission of the zinc finger peptides was observed through a 360 nm interference filter (10 nm bandwidth).

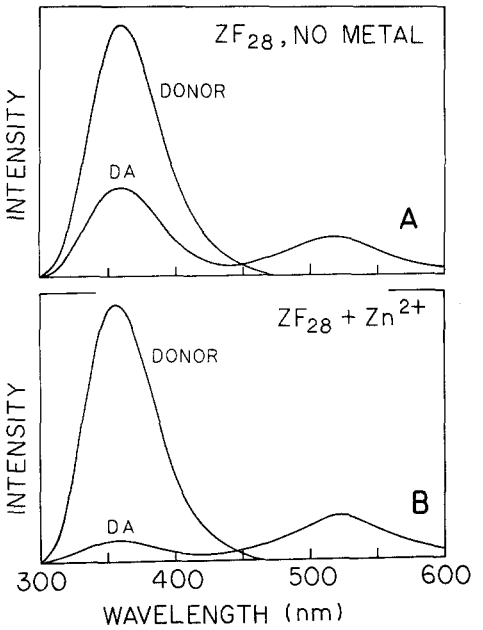

Fig. 1. (A) The steady-state emission spectra of metal-free ZF_{28} (donor) and dansylated ZF_{28} (D-A pair). (B) The steady-state emission spectra of zinc-bound ZF_{28} and dansylated ZF_{28}. The excitation wavelength was 295 nm.

RESULTS AND DISCUSSION

We chose to investigate a single-domain zinc finger peptide which is representative of the type found in eukaryotic transcription factors (CCHH) [4]. The peptide sequence of consensus peptide ZF_{28}, shown in Scheme I, is based on the consensus peptide work of Berg and co-workers [17].

The energy transfer donor (D) in ZF_{28} is a single tryptophan (W) located at the midpoint of the peptide sequence and the energy acceptor (A) is the DNS group attached at the amino terminus. Unlabeled peptide serves as the donor-only molecule and dansylated peptide serves as the D-A molecule. Zinc-coordinating residues are a pair of cysteines located at positions 4 and 7 and a pair of histidines located at positions 20 and 24. The approximate distance between TRP_{14} and the N-terminal DNS group, estimated from molecular graphics using the NMR-determined coordinates of Lee *et al.* [6], is 10 Å.

Steady-state fluorescence emission spectra of ZF_{28} donor-only peptide and DNS-ZF_{28} D-A peptide (Fig. 1) were measured with and without zinc ion. The tryptophan fluorescence in zinc-bound DNS-ZF_{28} (Fig. 1B) is significantly more quenched than that in metal-free DNS-ZF_{28} (Fig. 1A). This high degree of donor quenching by the acceptor indicates a higher overall energy transfer rate when zinc is bound. Based on these spectra, one can conclude that the mean D-A distance is shorter for the zinc-bound peptide than for the metal-free peptide.

Metal-free and zinc-bound ZF_{28} and DNS-ZF_{28} were also measured using time-resolved frequency-domain fluorometry. The frequency response curves, shown in Fig. 2, consist of both the phase angle shift and the modulation exhibited by the TRP_{14} donor. The donor-alone and D-A data were fit with a multiexponential lifetime model (Table I). The intensity decays of the donor both in the absence and presence of the acceptor and in the absence and presence of zinc were found to be heterogeneous. The triple-exponential model was needed for an adequate fit (Table I). For the donor-only peptide the presence of bound zinc shortens the decay time of the donor and decreases the tryptophan quantum yield. The yield (ϕ_D) were measured relative to that of tryptophan in water (ϕ_D = 0.13), [41] and were found to be 0.11 and 0.14 for the zinc ZF_{28} and metal-free ZF_{28}, respectively.

The presence of the DNS acceptor results in a dramatic decrease in the TRP_{14} donor decay time. This is

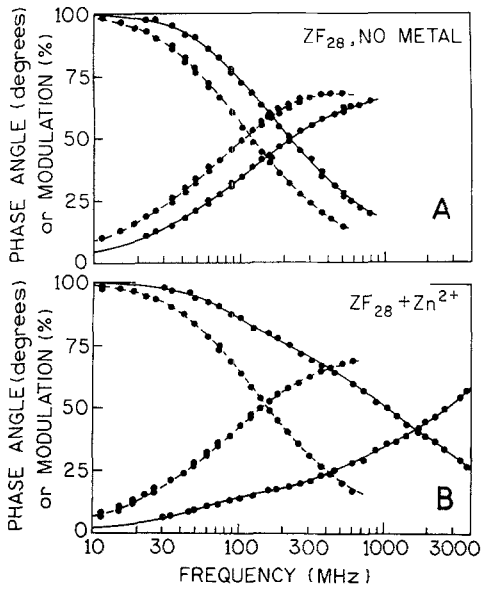

Fig. 2. (A) The multiexponential lifetime fits to the frequency-domain data for metal-free donor-only and donor-acceptor ZF_{28} peptides. (B) The multiexponential lifetime fits to the frequency-domain data for zinc-bound donor only and donor–acceptor ZF_{28} peptides. For both metal-free and zinc-bound conditions the donor–acceptor frequency response curves are shifted to higher frequencies.

seen from the mean lifetime (Table I) and by the shift in the frequency response curves to high frequencies, indicating that the donor fluorescence is quenched by the presence of acceptor. The TRP_{14} average donor lifetime is decreased about two-fold by the DNS acceptor in metal-free peptide (Fig. 2A), whereas in the zinc-bound peptide it is more highly quenched by acceptor (Figure 2B) as evidenced by the shift in the frequency response curves to much higher frequencies. These data confirm the steady-state results (Fig. 1), which indicated a much shorter D-A distance in zinc-bound ZF_{28} than that found in metal-free ZF_{28}.

The donor-to-acceptor distance distributions, which are assumed to be Gaussian, were determined from the frequency-domain data with and without mutual donor-to-acceptor diffusion (D), according to Eqs. (1)–(8). Since the zinc finger peptides were measured in buffer at 20°C, a temperature at which a significant amount of diffusion can occur between the donor and the acceptor, the correct distance distribution analysis is one that includes D. However, comparison of analyses which are performed using both models can verify the presence of diffusion. We note that the apparent static distributions are narrowed and generally shortened by donor-to-acceptor diffusion [30–33].

The TRP_{14}-to-N terminal DNS distance distributions for ZF_{28} are shown in Fig. 3 and reported in Table II. It is assumed that an average orientation ($\kappa^2 = 2/3$) exists between the donor and the acceptor chromophores; previous time-resolved measurements on the protein troponin [26] indicate that this is a valid assumption since the anisotropy-determined minimum and maximum values of κ^2 had only a small effect on the calculated values of R_{av} and hw and were not noticeably skewed to favor one orientation over another. A distance distribution not only gives the average D-A distance (R_{av}), but also indicates the degree of conformational freedom

Table I. Multiexponential Analysis of the Frequency-Domain Intensity Decays of the TRP_{14} Donor in the ZF_{28} Peptide and in the DNS-ZF_{28} Peptide

Sample	Condition	$< \tau >$ (ns)[a]	τ_i (ns)	α_i	f_i[b]	χ_R^2 (3 exp)
ZF_{28} +	No metal	2.47	0.040	0.662	0.035	4.84[c]
			1.60	0.260	0.558	
			3.90	0.078	0.407	
	Zn^{2+}	1.90	0.214	0.361	0.067	1.99
			1.31	0.504	0.569	
			3.12	0.135	0.363	
DNS-ZF_{28} +	No metal	1.28	0.002	0.945	0.033	4.61
			0.403	0.026	0.183	
			1.54	0.029	0.785	
	Zn^{2+}	0.58	0.048	0.774	0.332	13.7
			0.203	0.206	0.374	
			1.67	0.020	0.294	

[a] Average lifetime, $< \tau > = \Sigma_i \alpha_i \tau_i^2 / \Sigma_i \alpha_i \tau_i$.

[b] The fractional intensity (f_i) of the ith component in the emission is given by $f_i = \alpha_i \tau_i / \Sigma_j \alpha_j \tau_j$.

[c] The experimental uncertainties were 0.2° in phase and 0.005 in modulation.

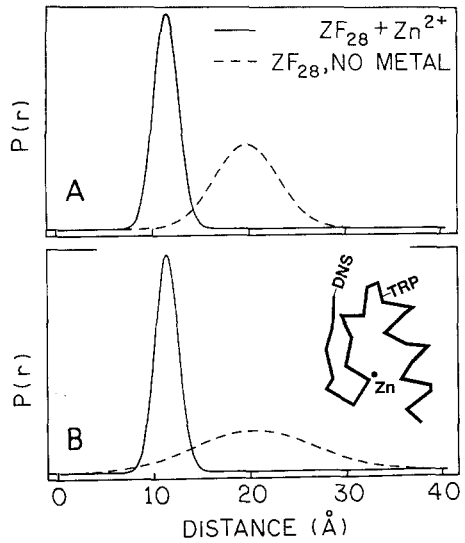

Fig. 3. Distance distributions calculated from the frequency-domain data for metal-free ZF_{28} and zinc-bound ZF_{28}. The distributions were analyzed with (B) and without (A) the apparent donor-to-acceptor diffusion coefficient. The inset in B shows a schematic representation of the zinc finger structure and the location of the tryptophan (TRP) donor and DNS acceptor (DNS).

(*hw*; full width of the distribution at half-maximum probability) that is present between the donor and the acceptor. Apparent distance distributions, i.e., calculated without consideration of the apparent site-to-site diffusion coefficient, are shown in Fig. 3A. As expected, the zinc-bound ZF_{28} D-A distance is shorter (R_{av} = 11.2 Å) and exhibits less conformational freedom (*hw* = 3.0 Å) than metal-free ZF_{28} (R_{av} = 19.4 Å, *hw* = 7.7 Å). Since the average D-A distance obtained for zinc-bound ZF_{28} is in close agreement with the corresponding distance (10 Å) from the NMR data, this suggests that the DNS group has not significantly perturbed the Zn finger structure [6].

Reanalysis of the data with the inclusion of the donor-to-acceptor diffusion coefficient [21, 22, 29–33] yields the distributions shown in Fig. 3B. One of the most notable observations is that the addition of this third parameter does not appreciably alter the calculated R_{av} or *hw* values (Table II) for the zinc-bound peptide. The apparent diffusion coefficient of 1.2×10^{-10} cm²/s for the zinc-bound peptide indicates that virtually no diffusion is occurring during the excited state of TRP_{14} (for a 2 ns tryptophan lifetime, the diffusive motion would be 0.06 Å) and that there is little D-A conformational freedom and no D-A flexibility when zinc is bound. This result is consistent with the assumption that the zinc finger structure adopts a stable and well-defined conformation upon binding zinc ion. The R_{av} value (20.1 Å) for the metal-free peptide is also nearly the same as that obtained without diffusion (19.4 Å). However, in contrast to the zinc-bound peptide, the width of the distribution (*hw* = 14.5 Å) is doubled when diffusion is considered in the analysis ($D = 1.2 \times 10^{-6}$ cm²/s).

Table II. Distance Distribution Parameters for ZF_{28}[a]

Conditions	R_{av} (Å)	*hw* (Å)	*D* (cm²/s)[b]	χ^2_{RN}
No metal	19.4	7.7	—	2.05
	(18.8–20.0)[c]	(7.3–8.1)		
	20.1	14.5	1.2×10^{-6}	1.02
	(19.5–20.7)	(12.3–19.5)	$(5.6 \times 10^{-7}$–$2.5 \times 10^{-6})$	
	20.2	14.6	$\langle 1.2 \times 10^{-6} \rangle$	1.00
	(19.6–20.8)	(12.4–19.6)		
Zinc ion	11.2	3.0	—	1.00
	(11.0–11.4)	(2.6–3.4)		
	11.2	2.8	1.2×10^{-10}	1.05
	(11.0–11.4)	(2.4–3.2)	$(0$–$1.3 \times 10^{-7})$	
	11.2	2.9	$\langle 2 \times 10^{-8} \rangle$	1.04
	(11.0–11.4)	(2.5–3.3)		

[a] R_{av} is the average D-A distance, *hw* is the full width at half-maximum of the distribution, *D* is the apparent donor-to-acceptor diffusion coefficient, and χ^2_{RN} is the normalized goodness-of-fit statistic. Values fixed during the fitting procedure are indicated by angle braces. Values in parentheses represent the 67% confidence intervals from the χ^2_R surfaces.

[b] 1×10^{-6} cm²/s = 10 Å²/ns.

[c] An apparent twofold smaller range of uncertainties is obtained if one uses the usual assumption of nonlinear least squares.

This result indicates the presence of considerable TRP_{14}-to-DNS diffusion (7 Å of diffusive motion would occur during a 2 ns lifetime) in the zinc-free peptide.

The information on the distance distributions and the rate of conformational interchange is contained within the frequency response curves shown in Fig. 2. It is natural to question whether these data are adequate to determine these molecular parameters and the range of uncertainty in the derived parameters. The range of uncertainty can be revealed by the $\chi^2_{R_N}$ surfaces of the distribution parameters R_{av}, hw, and log D (Fig. 4). The least-squares goodness-of-fit parameter ($\chi^2_{R_N}$) is in this case normalized to unity at its lowest value. These surfaces, generated by fixing one parameter and fitting to the other two parameters, provide a graphical representation of the uncertainty present in each determined parameter. The R_{av} and hw $\chi^2_{R_N}$ surfaces (Fig. 4A) for zinc-bound ZF_{28} (—) indicate that these two parameters are very well determined. For metal-free peptide (---) R_{av} is well determined; however, there is some degree of uncertainty in the value of the hw. The diffusion parameter (D) $\chi^2_{R_N}$ surfaces for zinc-bound (—) and metal-free (---) peptide are shown in Fig. 4B. The 67% confidence intervals for the diffusion parameter for metal-free ZF_{28} yield a range of 8–18 Å²/ns, which in our experience [43] is a good determination of this parameter. These confidence limits are summarized in Table II. For zinc-bound peptide one can see that we are limited in our ability to measure very low levels of diffusion. At the upper 67% confidence limit D = 1.6 Å²/ns. At this low level of diffusion, one can conclude that intramolecular motion for the zinc finger peptide in solution is essentially frozen out by the presence of zinc ion.

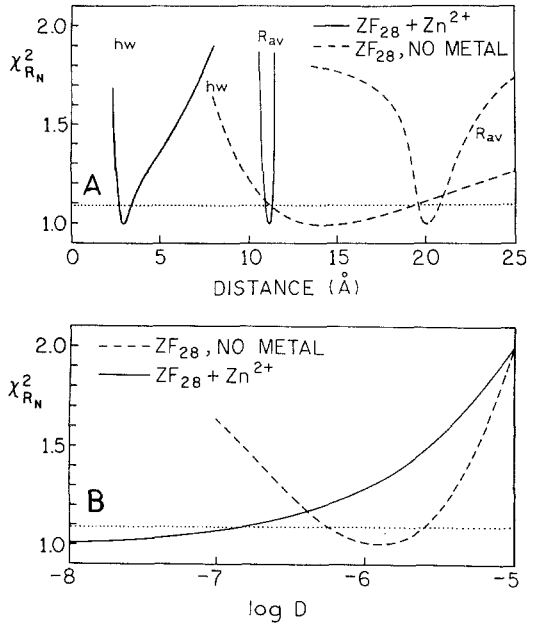

Fig. 4. Normalized χ^2_{RN} surfaces calculated for distance distributions analyzed with diffusion. These surfaces are generated by calculating the distance distribution with one parameter fixed and fitting to the other parameters. (A) The zinc-bound ZF_{28} (—) and metal-free ZF_{28} (---) χ^2_{RN} surfaces for R_{av} and hw. (B) The normalized χ^2_{RN} surfaces generated for log D (D is expressed as cm²/s; alternatively, 1×10^{-6} cm²/s = 10 Å²/ns). In both A and B the dotted line represents the 67% confidence interval.

Preliminary measurements (data not shown) of metal-free peptide in the presence of the denaturant guanidine hydrochloride (GuHCl) yield even larger R_{av} and hw values than those obtained for metal-free peptide alone. Assuming that GuHCl induces a random coil conformation in proteins, these larger R_{av} and hw values imply that there is probably some residual secondary/tertiary structure present in the absence of metal ion. This result is not entirely consistent with previous circular dichroism results [3, 5] on zinc finger peptides, which did not show the presence of any significant amount of secondary structure in the absence of metal ion. Our result is also at variance with a recent NMR study in which the authors concluded that the metal-free peptide exhibits chemical shifts (^1H and ^{13}C) very close to the random coil values [15]. It is possible that our method detects changes in structure which are not observed by other methods, assuming that these observed differences in the zinc finger distance distributions with and without GuHCl are not the result of nonspecific effects such as charge neutralization by the salt. For example, a small amount of molten globule structure [44,45] may affect the observed distance distribution but may not yield observable features in the CD spectra. Conversely, it might also be expected that close association of two or several amino acids may be apparent in the NMR spectra but may not yield a significant effect on the distance distribution. Finally, we note that our peptide may exhibit somewhat different behavior than the peptides used in other studies. The combined use of energy transfer distance distributions with the two-dimensional NMR data may provide additional insights into the solution conformation and dynamics of the zinc finger peptide.

We also questioned whether there existed a fraction of the donor–acceptor pairs which were closely spaced, for which energy transfer was complete, and thus which do not contribute to the intensity decay of the donor. Such a population of conformations could be detected by a decrease in the intensity (relative quantum yield) of the donor, compared to that predicted from the time-

resolved energy transfer data. The relative donor quantum yields can be estimated from Fig. 1 and used to estimate the transfer efficiency E_T.

In the absence and presence of bound Zn^{2+} the steady-state transfer efficiencies are 64 and 95%, respectively. The transfer efficiencies can also be estimated from the time-resolved frequency-domain data using

$$E_T = 1 - \frac{\int_0^\infty I_{DA}(t)\,dt}{\int_0^\infty I_D(t)\,dt} \qquad (15)$$

In the absence and presence of Zn, the transfer efficiencies were found to be 55 and 95%, respectively. The reasonable agreement between these transfer efficiencies excludes the possibility of a large fraction of the donor population being immediately adjacent to an acceptor.

Our data clearly show that zinc induces a stable, well-defined conformation in the consensus zinc finger peptide, whereas the metal-free peptide exhibits a greater degree of conformational flexibility. Additional evidence for the stability of the zinc-bound peptide is that there is very little change in the steady-state donor intensity when up to 8 *M* GuHCl is added to a D-A sample which contains zinc (data not shown), whereas a significant change in the donor intensity is observed for a metal-free peptide solution when 3 *M* GuHCl is added. The inclusion of a diffusion parameter in the distance distribution analysis emphasizes these conclusions since no improvement in χ^2_{RN} is obtained in the fit for zinc-bound peptide when diffusion in included. While we are aware that there is some amount of uncertainty in the determination of these distance distribution parameters when diffusion is included, the results obtained here are consistent with what is already known about the behavior of zinc finger peptides when metal is bound.

ACKNOWLEDGMENTS

J.R.L. acknowledges NIH Grant GM 35154 and support for instrumentation from NSF Grant DIR-8710401 and NIH Grant RR-08119. P.E. was supported (in part) by a Graduate Research Assistantship award from the UMAB Designated Research Initiative Fund. Mass spectral measurements were carried out at the Structural Biochemistry Center at the University of Maryland Baltimore County, a NSF-supported Biological Instrumentation Center. P.E. thanks H. Szmacinski, I. Gryczynski, and H. Malak for their expert assistance with the frequency-domain measurements. P.E. and J.R.L. thank Professors J. Collins and J. Theibert for the amino acid analysis and P. Wright and co-workers for the coordinates from their NMR-determined structure. P.E. also acknowledges J. Berg and co-workers at Johns Hopkins University for their helpful suggestions concerning the design of the zinc finger peptide.

A preliminary report on this topic was presented at the conference on Time-Resolved Laser Spectroscopy in Biochemistry III (SPIE, Vol. 1640, pp. 532–541, 1992).

REFERENCES

1. J. Miller, A. D. McLachlan, and A. Klug (1985) *EMBO J.* **4**, 1609–1614.
2. R. S. Brown, C. Sander, and P. Argos (1985) *FEBS Lett.* **186**, 271–274.
3. A. D. Frankel, J. M. Berg, and C. O. Pabo (1987) *Proc. Natl. Acad. Sci. USA* **84**, 4841–4845.
4. P. F. Johnson and S. L. McKnight (1989) *Annu. Rev. Biochem.* **58**, 799–839.
5. G. Párraga, S. J. Horvath, A. Eisen, W. E. Taylor, L. Hood, E. T. Young, and R. E. Klevit (1988) *Science* **241**, 1489–1492.
6. M. S. Lee, G. P. Gippert, K. V. Soman, D. A. Case, and P. E. Wright (1989) *Science* **245**, 635–637.
7. G. Párraga, S. Horvath, L. Hood, E. T. Young, and R. E. Klevit (1990) *Proc. Natl. Acad. Sci. USA* **87**, 137–141.
8. R. E. Klevit, J. R. Herriott, and S. J. Horvath (1990) *Proteins Struct. Funct. Genet.* **7**, 215–226.
9. M. A. Weiss, K. A. Mason, C. E. Dahl, and H. T. Keutmann (1990) *Biochemistry* **29**, 5660–5664.
10. J. G. Omichinski, G. M. Clore, E. Appella, K. Sakaguchi, and A. M. Gronenborn (1990) *Biochemistry* **29**, 9324–9334.
11. M. A. Weiss and H. T. Keutmann (1990) *Biochemistry* **29**, 9808–9813.
12. D. Neuhaus, Y. Nekaseko, K. Nagai, and A. Klug (1990) *FEBS Lett.* **626**, 179–184.
13. M. Kochoyan, T. F. Havel, D. Nguyen, C. E. Dahl, H. T. Keutmann, and M. A. Weiss (1991) *Biochemistry* **30**, 3371–3386.
14. M. Kochoyan, H. T. Keutmann, and M. A. Weiss (1991) *Biochemistry* **30**, 7063–7072.
15. M. S. Lee, J. M. Gottesfeld, and P. E. Wright (1991) *FEBS Lett.* **279**, 289–294.
16. M. Kochoyan, H. T. Keutmann, and M. A. Weiss (1991) *Biochemistry* **30**, 9396–9402.
17. B. A. Krizek, B. T. Amann, V. J. Kilfoil, D. L. Merkle, and J. M. Berg (1991) *J. Am. Chem. Soc.* **113**, 4518–4523.
18. J. M. Berg (1988) *Proc. Natl. Acad. Sci. USA* **85**, 99–102.
19. N. P. Pavletich and C. O. Pabo (1991) *Science* **252**, 809–817.
20. E. Haas, H. Wilchek, E. Katchalski-Katzir, and I. Z. Steinberg (1975) *Proc. Natl. Acad. Sci. USA* **72**, 1807–1811.
21. E. Haas, E. Katchalski-Katzir, and I. Z. Steinberg (1978) *Biopolymers* **17**, 11–31.
22. E. Haas and I. Z. Steinberg (1984) *Biophys. J.* **46**, 429–437.
23. D. Amir and E. Haas (1986) *Biopolymers* **25**, 235–240.
24. J. R. Lakowicz, M. L. Johnson, W. Wiczk, A. Bhat, and R. F. Steiner (1987) *Chem. Phys. Lett.* **138**, 587–593.
25. J. R. Lakowicz, I. Gryczynski, H. C. Cheung, C. K. Wang, and M. L. Johnson (1988) *Biopolymers* **27**, 821–830.
26. J. R. Lakowicz, I. Gryczynski, H. C. Cheung, C. K. Wang, M. L. Johnson, and N. Joshi (1988) *Biochemistry* **27**, 9149–9160.
27. J. M. Beechem and E. Haas (1989) *Biophys. J.* **55**, 1225–1236.

28. J. R. Lakowicz, I. Gryczynski, W. Wiczk, G. Laczko, F. G. Prendergast, and M. L. Johnson (1990) *Biophys. Chem.* **36**, 99–115.
29. E. Haas, C. A. McWherter, and H. A. Scheraga (1988) *Biopolymers* **27**, 1–21.
30. J. R. Lakowicz, J. Kuśba, W. Wiczk, I. Gryczynski, and M. L. Johnson (1990) *Chem. Phys. Lett.* **173**, 319–326.
31. J. R. Lakowicz, J. Kuśba, I. Gryczynski, W. Wiczk, H. Szmacinski, and M. L. Johnson (1991) *J. Phys. Chem.* **95**, 9654–9660.
32. J. R. Lakowicz, J. Kuśba, W. Wiczk, I. Gryczynski, H. Szmacinski, and M. L. Johnson (1991) *Biophys. Chem.* **39**, 79–84.
33. J. R. Lakowicz, J. Kuśba, H. Szmacinski, I. Gryczynski, P. S. Eis, W. Wiczk, and M. L. Johnson (1991) *Biopolymers* **31**, 1363–1378.
34. L. Stryer (1978) *Annu. Rev. Biochem.* **47**, 819–846.
35. J. Kuśba and J. R. Lakowicz (1993) *Methods Enzymology; Numerical Computer Methods, Part B,* in press.
36. M. L. Johnson (1985) *Anal. Biochem.* **148**, 471–478.
37. M. Straume, S. G. Frasier-Cadoret, and M. L. Johnson (1991) in J. R. Lakowicz (Ed.), *Topics in Fluorescence Spectroscopy, Vol. 2. Principles,* Plenum Press, New York, pp. 177–240.
38. J. R. Lakowicz, E. Gratton, G. Laczko, H. Cherek, and M. Limkeman (1984) *Biophys. J.* **46**, 463–477.
39. E. Gratton, J. R. Lakowicz, B. Maliwal, H. Cherek, G. Laczko, and M. Limkeman (1984) *Biophys. J.* **46**, 479–486.
40. P. S. Eis and J. R. Lakowicz (1992) Time-resolved laser spectroscopy in biochemistry III. *SPIE* **1640**, 532–541.
41. R. F. Chen (1967) *Anal. Lett.* **1**, 35–42.
42. J. R. Lakowicz, G. Laczko, and I. Gryczynski (1986) *Rev. Sci. Instrum.* **57**, 2499–2508.
43. J. R. Lakowicz, I. Gryczynski, J. Kuśba, W. Wiczk, H. Szmacinski, and M. L. Johnson, unpublished observation.
44. P. S. Kim and R. L. Baldwin (1982) *Annu. Rev. Biochem.* **51**, 459–489.
45. P. S. Kim and R. L. Baldwin (1990) *Annu. Rev. Biochem.* **59**, 631–660.